Metallomics

PAPER

View Article Online
View Journal | View Issue

Cite this: *Metallomics*, 2015, 7, 567

A set of robust fluorescent peptide probes for quantification of Cu(II) binding affinities in the micromolar to femtomolar range†

Tessa R. Young, Chathuri J. K. Wijekoon, Benjamin Spyrou, Paul S. Donnelly, Anthony G. Wedd and Zhiguang Xiao*

Reliable quantification of copper binding affinities and identification of the binding sites provide a molecular basis for an understanding of the nutritional roles and toxic effects of copper ions. Sets of chromophoric probes are now available that can quantify Cu(I) binding affinities from nanomolar to attomolar concentrations on a unified scale under *in vitro* conditions. Equivalent probes for Cu(II) are lacking. This work reports development of a set of four fluorescent dansyl peptide probes (DP1–4) that can quantify Cu(II) binding affinities from micromolar to femtomolar concentrations, also on a unified scale. The probes were constructed by conjugation of a dansyl group to four short peptides of specific design. Each was characterised by its dissociation constant K_D, its pH dependence and the nature of its binding site. One equivalent of Cu(II) is bound by the individual probes that display different and well-separated affinities at pH 7.4 ($\log K_D$ = −8.1, −10.1, −12.3 and −14.1, respectively). Intense fluorescence is emitted at λ_{max} ~ 550 nm upon excitation at ~330 nm. Binding of Cu(II) quenches the fluorescence intensity linearly until one equivalent of Cu(II) is bound. Multiple approaches and multiple affinity standards were employed to ensure reliability. Selected examples of application to well-characterised Cu(II) binding peptides and proteins are presented. These include Aβ16 peptides, two naturally occurring Cu(II)-chelating motifs in human serum and cerebrospinal fluid with sequences GHK and DAHK and two copper binding proteins, CopC from *Pseudomonas syringae* and PcoC from *Escherichia coli*. Previously reported affinities are reproduced, demonstrating that peptides DP1–4 form a set of robust and reliable probes for Cu(II) binding to peptides and protein targets.

Received 19th November 2014,
Accepted 11th February 2015

DOI: 10.1039/c4mt00301b

www.rsc.org/metallomics

Introduction

Copper is a redox-active metal whose relevant oxidation states Cu(I) and Cu(II) bind with high affinities to many sites in biomolecules. These properties confer vital roles in cellular respiration, antioxidant defense, iron uptake, connective tissue formation, pigment synthesis and photosynthesis.[1] However, when not under proper control, these same properties render copper toxic to cells. Then, undesirable redox chemistry may lead to catalytic generation of reactive oxygen species (ROS) while the dominant affinities result in displacement of other essential metals from their native sites. Consequently, a delicate balance must be maintained between deficiency and excess and specific homeostatic mechanisms have evolved to control copper metabolism.[2–4] Errors in cellular copper handling appear to contribute to a range of inherited and acquired diseases. Genetic mutations invoke Menkes' and Wilson's diseases, conditions of, respectively, copper deficiency and overload. A range of neurodegenerative diseases have been linked to aberrant copper metabolism and include Alzheimer's, prion and Parkinson's diseases.[5–9]

Reliable quantitative evaluation of copper–protein interactions for relevant oxidation states provides an essential key to understanding the molecular basis of nutritional roles and toxic effects. Such evaluation must be based on a combination of reliable affinity standards and sensitive detection probes.[10] We have previously established a set of classic chromophoric ligands that are capable of quantifying Cu(I) binding in proteins with affinities within the range from nanomolar to attomolar concentrations in *in vitro* systems.[11–15] Their establishment has unified the scattered literature data to a single affinity scale.[10,13,15] Promising alternative probes for Cu(I) have been developed.[16]

In contrast, quantitative evaluation of binding affinities for Cu(II) sites in proteins and peptides currently rely largely on competition with a range of non-chromophoric ligands including those based on polydentate amine carboxylates such as ethylenediaminetetraacetate (Edta), ethylene glycol tetraacetate (Egta), *N*-(2-hydroxyethyl)ethylenediamine-*N*,*N*′,*N*′-triacetate (Hedta) and

School of Chemistry and The Bio21 Molecular Science and Biotechnology Institute, University of Melbourne, Parkville, Victoria 3010, Australia.
E-mail: z.xiao@unimelb.edu.au; Fax: +61 3 9347 5180; Tel: +61 3 9035 6072

† Electronic supplementary information (ESI) available: Characterisation of probes DP1-4; Table S1; eqn (S1) and (S2); Fig. S1–S6. See DOI: 10.1039/c4mt00301b

nitrilotriacetate (Nta) or amino acids such as glycine (Gly) and histidine (His).[10] However, whilst the affinities of these ligands are well-documented, their Cu(II) complexes are 'invisible' and cannot act as direct detection probes. Their use depends upon observation of a change in an inherent property of the protein target itself upon the binding of Cu(II) (fluorescence, absorbance, circular dichroism).[10,17] The availability of such properties depends on the target itself.

Isothermal titration calorimetry (ITC) has been employed extensively as a detection probe.[18] The approach relies on the measurement of the heat generated during the course of metal-binding but suffers in complex systems from interfering heat release from accompanying processes such as dilution, precipitation or the presence of (unappreciated) competing ligands such as buffers. In addition, time constraints between the consecutive ITC titrations can be limiting as Cu(II) transfer tends to be sluggish. Such aspects seem to account for the scattered literature data for Cu(II) binding affinities, as highlighted by the cases of protein domains or peptides associated with neurodegenerative diseases.[17] Consequently, there remains a need for reliable probes capable of direct quantification of Cu(II) binding with high sensitivity.

Recently, the Aβ16 peptide was modified by replacement of Tyr10 with the fluorescent Trp residue.[19] This system proved to be a useful probe for differentiating the Cu(II) binding affinities of different forms of the Aβ peptide. However, it appears to be subject to interference from binding of a second equivalent of Cu(II) to a weaker binding site. The system was converted to a more sensitive and selective probe (denoted as Aβ16wwa) by replacement of Phe4 with Trp and His14 with Ala (conditional $\log K_D = -9.8$ at pH 7.4).[20] However, the use of Aβ16wwa is also limited due to an interfering response from those protein targets that also contain Trp residues plus an 'inner filter' effect of Cu(II) species at ~280 nm, its optimal excitation wavelength.

Fluorescent probes for Cu(II) with red-shifted excitation have been reported (see recent reviews[21,22]) including several containing one or two sensitive dansyl groups (DNS) attached to primary amine group(s) in an amino acid or a short peptide,[23–26] as well as several biosensors based on fluorescence-labelled carbonic anhydrases.[27,28] However, these probes were either not demonstrated to be practical for quantification of Cu(II) affinities in biomolecules or not readily available for the practical applications.

This paper reports a set of four new sensitive and quantitative probes for Cu(II) that were constructed by conjugation of DNS to four different short peptides. They each bind one equiv. of Cu(II) cleanly with varying binding modes, binding affinities and pH dependency and are able to probe Cu(II) binding sites and define Cu(II) binding affinities from micromolar to femtomolar concentrations on a unified scale. Examples of their application to peptide and protein targets are provided.

Experimental section

Materials and general procedure

Ligands Gly, His, Egta, Edta and Hedta were purchased from Sigma-Aldrich and were used as received. Concentrations of Egta, Edta and Hedta were calibrated *via* Cu(II) titration into a mixture of ligand and probe DP2 (*cf.* Fig. 9 below). A Cu(II) standard was prepared by dissolving $CuSO_4$ in Milli-Q water and its concentration calibrated *via* reaction with excess Cu(I) ligand bathocuproïne disulfonate (Bcs) in buffer 3-(*N*-morpholino)propanesulfonate (MOPS) containing reductant NH_2OH. Under such conditions, all copper ions were converted quantitatively to the well-defined chromophoric complex anion $[Cu^I(Bcs)_2]^{3-}$ with a strong absorbance at 483 nm (ε = 13 000 M^{-1} cm^{-1}).[12] Proteins CopC from *Pseudomonas syringae* and PcoC from *Escherichia coli* were expressed and isolated as reported.[29,30] Their concentrations were estimated from their solution absorbances at 280 nm using reported extinction coefficients of $\varepsilon(280)$ = 8700 and 10 100 M^{-1} cm^{-1}, respectively.[29,30] Peptides Aβ16 (amyloid-β peptide: DAEFRHDSGYEVHHQK), Ac-Aβ16 (N-terminus acetylated) and Aβ16wwa (sequence: DAEWRHDSGWEVHAQK) were synthesised on site by solid phase peptide techniques. Identity was verified by electrospray ionisation mass spectrometry (ESI-MS) while purity was confirmed by HPLC to be >98%. Peptide concentrations were estimated from absorbance maxima at ~276 nm using ε_{max} = 1410 M^{-1} cm^{-1} for those Aβ16 peptides containing a single tyrosine residue and ε = 11 000 M^{-1} cm^{-1} at 280 nm for the Aβ16wwa peptide containing two Trp residues. The concentrations obtained matched those estimated from fluorescence titrations with the copper standard assuming formation of a 1 : 1 complex in each case.

The four peptide probes listed in Table 1 were custom synthesised by GL Biochem (Shanghai), together with two shorter peptides with sequences GHK and DAHK. The dansyl fluorophore was introduced at the ε-amino group of the sole lysine residue in the sequence (denoted as K^{DNS}; Fig. 1) using Fmoc-L-Lys(dansyl)-OH. The identity and purity (>98%) of each probe was confirmed by ESI-MS and HPLC (Table 1). The solution spectrum of each probe features an intense absorbance in the near UV region with λ_{max} = 326 nm, characteristic of a single dansyl group (*cf.*, Fig. 2, cyan trace for DP1–4 *versus* orange trace for DAHK). The maximal molar extinction coefficient at 326 nm was determined accurately *via* titration of each probe solution with a $CuSO_4$ standard (Fig. S2, ESI†) to be 4500 M^{-1} cm^{-1} for each probe. This value is within the range reported previously for several dansyl derivatives[31,32] and was used in this work to calibrate the probe concentration. The concentrations of GHK and DAHK were determined *via*

Table 1 Properties of probes DP1–4

Probe	Sequence	Net charge[a]	Molar mass (Da) Calcd	Molar mass (Da) Found	(F_1/F_0) at given pH[b] 6.2	7.4	9.2
DP1	Ac-DH(K^{DNS})HD	−3	925.9	925.3	—	0.15[c]	0.06
DP2	DAE(K^{DNS})RHDH	−2	1240.3	1240.5	0.22	0.17	0.17
DP3	HP(K^{DNS})DHDH	−2	1118.2	1118.4	0.13	0.13	0.13
DP4	H(K^{DNS})HH	0	790.8	791.3	0.09	0.09	0.09

[a] At pH 7.4. [b] F_1 and F_0 are the fluorescence intensities upon binding 1.0 and 0.0 equiv. of Cu(II), respectively, under the same pH conditions and the F_1 values were determined directly from the titration turning point unless otherwise indicated. [c] This F_1 value was obtained from the best curve fitting of the experimental data to eqn (4) (see Fig. 4b).

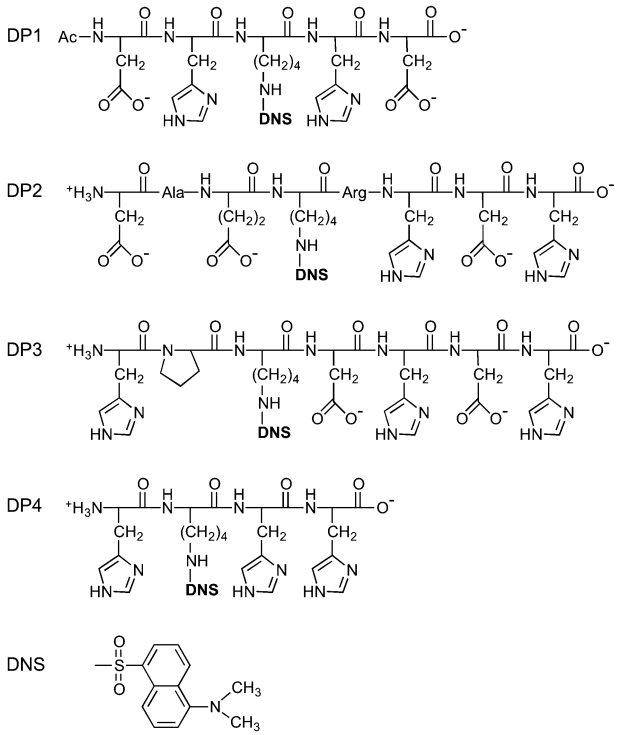

Fig. 1 DP probe peptides used in this study and structure of dansyl probe.

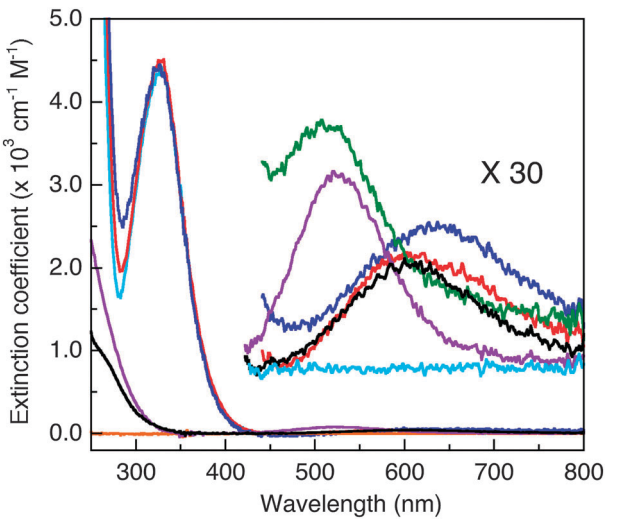

Fig. 2 Solution absorbance spectra in MOPS buffer (50 mM, pH 7.4). Cyan: *apo*-DP1–4; blue: Cu^{II}–DP2; red: Cu^{II}–DP3; green: Cu^{II}–DP4 (overlapping the blue trace of Cu^{II}–DP2 between 250–400 nm); orange: *apo*-GHK or *apo*-DAHK (no detectable absorbance at $\lambda > 250$ nm); black: Cu^{II}–GHK; purple: Cu^{II}–DAHK. The spectra in the visible region were scaled up by a factor of 30 to highlight an absorbance maximum around 525 nm that is a fingerprint for the presence of a Cu(II) centre in the ATCUN binding mode.

titration with the $CuSO_4$ standard using DP2 as a probe (*vide infra*; Fig. 9).

The experimental results were highly dependent on pH. To ensure accuracy and reliability, the solution pH was controlled within ±0.05 pH units and checked before and after each experiment.

Spectroscopic approaches

UV-visible spectra were recorded on a Varian Cary 300 spectrophotometer in dual beam mode with quartz cuvettes of 1.0 cm path length. All titrations with metal ions were performed in appropriate buffers and corrected for baseline and dilution. Fluorescence emission spectra were recorded on a Varian Cary Eclipse spectrophotometer with a band pass of 20 nm for both excitation and emission. The excitation wavelength for the dansyl probes was λ = 330 nm and the emission spectra were recorded between λ = 450–750 nm at a scale rate of λ = 600 nm min^{-1}. The excitation wavelength for other peptides or proteins was 280 nm with a recorded spectral range between 295–500 nm. Visible CD spectra were recorded on a Chirascan-plus spectrometer (Applied Photophysics) using a 1.0 cm cell. Three scans were averaged and a baseline was subtracted from each recorded spectrum.

Electron paramagnetic resonance (EPR) spectra were recorded on Bruker Elexsys E 500 EPR spectrometer. The samples were prepared by adding 0.9 equivalent Cu(II) into apo-peptides (each 0.5 mM) in an appropriate buffer (50 mM) containing ~10% glycerol. The samples were snap-frozen in liquid nitrogen and the spectra recorded at 77 K in a liquid-nitrogen finger Dewar. The EPR parameters (g values and A values) were extracted directly from the recorded spectra.

Quantification of Cu(II) binding *via* direct metal ion titration

Each DP probe emits intense fluorescence at $\lambda_{max} \sim 550$ nm upon excitation at ~330 nm. Cu(II) binding quenches the fluorescence intensity linearly until the binding site(s) are saturated with Cu(II). The binding stoichiometry was determined in each case by direct titration of the probe solution (2.0 mL) in an appropriate buffer with a $CuSO_4$ standard at a concentration 40 times that of the probe. For those probes with weaker Cu(II) affinity, the titration was conducted with high probe concentration and/or in a buffer with elevated pH to promote quantitative binding of the added Cu_{aq}^{2+} ions to achieve better definition of the titration turning point.

When the titration was conducted with lower probe concentration, the turning point may become less well-defined, suggesting the existence of a binding equilibrium (eqn (1)) under the constraint of $K_D' \sim [P]$ and thus $[Cu^{II}P]/[Cu(II)]_{tot} < 1$ in eqn (2):[20]

$$Cu_{aq}^{2+} + 2P + \text{'}Cu^{II}B\text{'} \rightleftharpoons 2Cu^{II}P + B \quad (1)$$

$$\frac{[Cu^{II}P]}{[Cu(II)]_{tot}} = \frac{[P]}{K_D(1 + K_A[B]) + [P]} = \frac{[P]}{K_D' + [P]} \quad (2)$$

K_A is the average association constant of the putative complex(es) Cu^{II}–B (B = buffer and all other potential Cu(II) ligands except H_2O) and K_D and K_D' are the conditional and the apparent dissociation constants of $Cu^{II}P$, respectively. K_D is dependent on solution pH only under the experimental conditions while K_D' (=$K_D(1 + K_A[B])$) is dependent on both pH and other conditions (such as competition from buffer, *etc.*, represented collectively by the term '$K_A[B]$').[17,33] Consequently, K_D' may vary between different experiments but will approach the conditional K_D when the term $K_A[B] \ll 1$. Nevertheless, under

the equilibrium conditions of $K_D' \sim [P]$, *i.e.*, $[Cu^{II}\text{–}P]/[Cu]_{tot} < 1.0$ (ideally within the range 0.2–0.8), the concentration of complex $[Cu^{II}P]$ in eqn (2) may be described *via* eqn (3) and consequently the relationship between F/F_0 and $[Cu]_{tot}/[P]_{tot}$ *via* eqn (4) on the basis of eqn (5):

$$[Cu^{II}P] = \frac{K_D' + [Cu]_{tot} + [P]_{tot} - \sqrt{(K_D' + [Cu]_{tot} + [P]_{tot})^2 - 4[Cu]_{tot}[P]_{tot}}}{2} \quad (3)$$

$$\frac{F}{F_0} = 1 + \left(\frac{1}{2}\right)\left(\frac{F_1}{F_0} - 1\right) \times \left(\frac{K_D'}{[P]_{tot}} + \frac{[Cu]_{tot}}{[P]_{tot}} + 1 - \sqrt{\left(\frac{K_D'}{[P]_{tot}} + \frac{[Cu]_{tot}}{[P]_{tot}} + 1\right)^2 - \frac{4[Cu]_{tot}}{[P]_{tot}}}\right) \quad (4)$$

$$\frac{[Cu^{II}P]}{[P]_{tot}} = \frac{F_0 - F}{F_0 - F_1} \quad (5)$$

$[Cu]_{tot}$ and $[P]_{tot}$ are the total concentrations of Cu(II) and probe P and F_0, F and F_1 are the fluorescence intensities of P when it binds 0.0, <1 and 1.0 equiv. of Cu(II), respectively. For a given probe, the value of F_1/F_0 may vary with buffer pH, but is fixed in a buffer of constant pH (Table 1). It was estimated at a probe concentration and/or a pH value that satisfied the condition $[P] \gg K_D'$, thereby ensuring high Cu(II) occupation of the probe at the titration equivalent point (*cf.*, eqn (2)). Therefore, K_D' may be estimated *via* curve-fitting of the experimental data to eqn (4). Alternatively, when F_1/F_0 cannot be defined reliably due to either weak binding or interference from a second Cu(II) binding site, both F_1/F_0 and K_D' was estimated *via* iterative variation of F_1/F_0 and K_D' in the curve-fitting of eqn (4) to optimise the fitting outputs. The potential impact of the reaction buffer on K_D' was evaluated according to the relationship $K_D = K_D'(1 + K_A[B])$ by varying the buffer concentrations.

Quantification of Cu(II) binding affinities *via* ligand competition

For those probes with a sufficiently high affinity for Cu(II), the condition $K_D' \sim [P]$ cannot be met even at the experimentally accessible minimal probe concentrations (*cf.* eqn (1) and (2)). Then, a competition for Cu(II) with a suitable ligand of well-defined Cu(II) binding affinity is required for reliable quantification. In this work, the classic Cu(II) ligands L = Gly, His, Egta and Hedta (Fig. S1, ESI†) were employed. The two amino acid ligands react with Cu(II) to yield both 1 : 1 and 1 : 2 complexes while the others form a 1 : 1 complex only with known formation constants (Table S1, ESI†). They may compete for Cu(II) with probes P according to eqn (6a) or (6b) under conditions where the contributions of free Cu_{aq}^{2+} and putative buffer complex 'Cu^{II}–B' to the total Cu(II) speciation are negligible. Then the free Cu_{aq}^{2+} concentration in the competing solutions may be estimated *via* eqn (7a) or (7b) and the pH-dependent conditional K_D for Cu^{II}–P derived *via* curve-fitting of the experimental data to eqn (8):[10]

$$Cu^{II}P + 3L \rightleftharpoons P + Cu^{II}L + Cu^{II}L_2 \text{ (L = Gly or His)} \quad (6a)$$

$$Cu^{II}P + L \rightleftharpoons P + Cu^{II}L \text{ (L = Egta or Hedta)} \quad (6b)$$

$$[Cu_{aq}^{2+}] = \frac{[Cu]_{tot} - [Cu^{II}P]}{K_{A1}[L] + K_{A1}K_{A2}[L]^2} \quad (7a)$$

$$[Cu_{aq}^{2+}] = \frac{[Cu]_{tot} - [Cu^{II}P]}{K_A[L]} \quad (7b)$$

$$\frac{[Cu^{II}P]}{[P]_{tot}} = \frac{[Cu_{aq}^{2+}]}{K_D + [Cu_{aq}^{2+}]} \quad (8)$$

K_A is the formation constant of the appropriate Cu(II) complex that is given in Table S1 (ESI†) and [L] is the equilibrium concentration of total ligand L species that do not bind Cu(II). The term [L] was calculated as detailed in ref. 10. The term $[Cu^{II}P]/[P]_{tot}$ in eqn (8) may be estimated *via* eqn (5) on the condition that the change in the fluorescence intensity of the competing solution in eqn (6a) or (6b) is dominated by the change in Cu(II) occupancy on the probe with negligible impact of possible inner-filter effects. Since buffer and other unknown components are assumed not to be involved in the competition for Cu(II) in eqn (6a) and (6b), the dissociation constant derived from eqn (8) is a pH-dependent conditional K_D that may be different from the apparent K_D' determined above *via* direct metal ion titration. The latter is more vulnerable to the impact of other solution conditions.

The experiments were conducted in buffers 2-(*N*-morpholino)-ethanesulfonate (MES, pH 6.2), MOPS (pH 7.4) and *N*-cyclohexyl-2-aminoethanesulfonate (CHES, pH 9.2), respectively, to derive the corresponding K_D values of each probe. The rates of reactions (6a) and (6b) vary considerably depending on the exact nature of P and L (Fig. S3, ESI†). Consequently, two experimental procedures were employed in this work:

Procedure I for faster reactions that take less than 10 min to reach equilibrium. Ligand L was titrated into a solution of probe complex Cu_x–DP ($x \leq 1.0$ to minimise the concentration of free Cu_{aq}^{2+} in solution). Cu(II) transfer after each titration was monitored by the recovery of the fluorescence intensity at 550 nm for the probe.[34] The Cu(II) occupancy of the probe can be estimated *via* eqn (5) and the corresponding free metal concentration $[Cu_{aq}^{2+}]$ calculated *via* eqn (7a) or (7b). Then, K_D values may be obtained *via* curve fitting of the derived data to eqn (8). This approach is subjected to the effects of titration dilution that, however, were controlled to a minimum by adjusting relevant concentrations and volumes.

Procedure II for slower reactions that take more than 10 min to reach equilibrium. A series of solutions were prepared that contained a fixed total concentration of the probe complex Cu_x–DP ($x \leq 1.0$) but varying total concentrations of competing ligand $[L]_{tot}$. Each solution was incubated separately until a stable fluorescence spectrum was recorded. Subsequent data

processing and analysis are identical to those of procedure I. There are no titration dilution effects in this approach.

Selected examples of applications

The four probes DP1–4 developed in this work bind Cu(II) with varying binding affinities and may be applied to quantify Cu(II)-binding properties (stoichiometry and affinity) of peptide/protein targets T (eqn (9)–(11)):

$$Cu^{II}P + T \rightleftharpoons Cu^{II}T + P \quad (9)$$

$$K_{ex} = \frac{[Cu^{II}T][P]}{[Cu^{II}P][T]} = \frac{K_D(P)}{K_D(T)} \quad (10)$$

$$\frac{[T]_{tot}}{[P]_{tot}} = \frac{[Cu]_{tot} - [Cu^{II}P]}{[P]_{tot}} + \frac{K_D(T)}{K_D(P)}\left(\frac{[Cu]_{tot}}{[Cu^{II}P]} - 1\right)\left(1 - \frac{[Cu^{II}P]}{[P]_{tot}}\right) \quad (11)$$

Eqn (11) is derived from eqn (10) with incorporation of mass balance relationships for an effective competition described by eqn (9) and is in a convenient format for curve-fitting of the experimental data to derive K_D(T) with known K_D(P). Under the conditions of the fluorescent emission of the dansyl probes (λ_{ex} = 330 nm; λ_{em} ~ 550 nm), the protein targets are generally fluorescence-silent and thus the Cu(II) speciation in eqn (9)–(11) may be analysed conveniently and reliably by monitoring the response of the probe to binding of Cu(II) *via* eqn (5).

For a target whose Cu(II) affinity is comparable or stronger than that of the probe, titration of Cu_{aq}^{2+} into a solution containing equimolar P and T quenched the probe fluorescence intensity until reaching a turning point at which the Cu(II) sites of both P and T were fully occupied. A control titration of the probe solution containing no protein target allowed determination of the stoichiometry of binding to the protein target since each probe is known to bind one equiv. of Cu(II) at the titration turning point (*vide infra*).

On the other hand, titration of a protein target into a solution containing the probe complex $Cu^{II}P$ may induce an effective competition satisfying eqn (9)–(11). The term [$Cu^{II}P$] may be determined directly *via* eqn (5) and then the protein K_D(T) can be estimated *via* curve-fitting of the experimental data to eqn (11) using the known K_D(P). The Cu(II)-exchange reaction of eqn (9) involving some targets is slow and takes ~1 h to reach equilibrium (Fig. S3, ESI†). In such cases, procedure II was adopted. Briefly, a series of solutions were prepared which contained a fixed total concentration of the probe complex Cu_x–P ($x \leq 1.0$) but varying total concentrations of target T in an appropriate buffer. Each solution was incubated until a stable fluorescence spectrum was reached (>1 h) and recorded. The data were compared and analysed to derive the affinity of the protein target as detailed above. The protein and peptide targets selected cover a wide range of affinities from micromolar to femtomolar and include Aβ-peptides Ac-Aβ16, Aβ16 and Aβ16wwa,[20] two naturally occurring Cu(II)-chelating motifs in human serum and cerebrospinal fluid with sequences GHK and DAHK,[33] and two copper binding proteins CopC from *Pseudomonas syringae* and PcoC from *Escherichia coli*.[29,30]

Results and discussion

Characterisation of the probes

Some common features. Four dansyl peptide probes DP1–4 were designed and developed in this work (Fig. 1 and Table 1). Solution spectra of metal-free forms in Mops buffer (50 mM, pH 7.4) were indistinguishable and were characterised by an intensive absorbance in the near UV region (λ_{max} = 326 nm; ε = 4500 cm^{-1} M^{-1}) attributable to the presence of a single dansyl group in each probe molecule (Fig. 2, cyan trace). The molar absorptivities ε were determined *via* titration of each probe with a Cu(II) standard (Fig. S2, ESI†) and lie within the reported range for a molecule conjugated with a single dansyl group.[31,32]

Titration of each probe with Cu_{aq}^{2+} induced minor increases in absorbance at ~280 nm (Fig. 2, red, blue traces), presumably arising from ligand-to-Cu(II) charge-transfer transitions. Absorbance changes were observed more clearly for the two dansyl-free Cu(II)–peptide complexes Cu^{II}–GHK and Cu^{II}–DAHK (Fig. 2, black and purple traces *versus* orange trace for *apo*-DAHK). The major absorbance at 326 nm assigned to the dansyl group remained essentially unchanged upon titration of Cu_{aq}^{2+} into the four DP probe solutions (Fig. 2), consistent with the binding sites accessed by Cu(II) in each DP probe involving ligands derived from the peptide, not from the dansyl group itself.

Weak absorbance peaks are seen in the visible region for the Cu(II) complexes, attributable to the Cu(II) d–d transitions. In particular, peaks at ~525 nm (ε ~ 100–20 M^{-1} cm^{-1})[35] were observed for both Cu^{II}–DP4 and Cu^{II}–DAHK (Fig. 2, green and purple traces), suggestive of the presence of a so-called amino terminal Cu and Ni binding motif (*i.e.*, ATCUN motif; see Fig. 3b).[36] DAHK is a naturally-occurring Cu(II)-binding tetrapeptide found in human serum and its ability to bind Cu(II) in the ATCUN binding mode has been documented convincingly.[37] Multiple additional pieces of evidence also support an ATCUN Cu(II) centre in Cu(II)–DP4 within the pH range 6.2–9.2 (Fig. 3b; *vide infra* and ESI†). Both peptides DP4 and DAHK possess the structural elements of the ATCUN motif: (i) a free N-terminus; (ii)

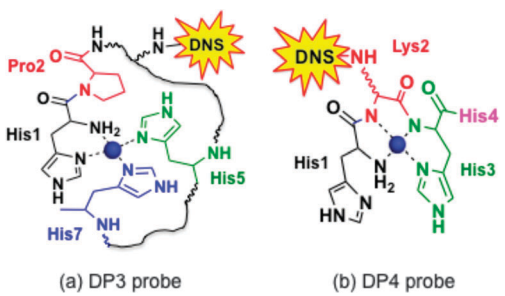

Fig. 3 Proposed equatorial Cu(II) ligands in DP3 (His–Pro–Lys^{DNS}–Asp–His–Asp–His) and DP4 (His–Lys^{DNS}–His–His). Possible axial coordination ligand(s) include carboxylate(s) from Asp4 and/or Asp6 in DP3 and imidazole nitrogen ligand(s) from His1 and/or His4 in DP4. DNS = dansyl flurophore.

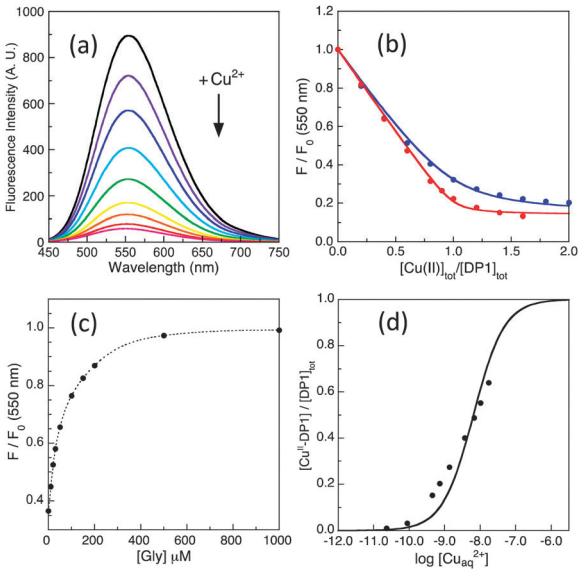

Fig. 4 Determination of apparent K_D' for Cu^{II}–DP1 by direct metal ion titration (a, b) and conditional K_D by ligand competition (c, d) in MOPS buffer (5.0 mM unless otherwise indicated, pH 7.4): (a) quenching of fluorescence emission intensity (λ_{max} = 550 nm) of *apo*-DP1 (2.0 μM) upon titration with Cu_{aq}^{2+} solution (80 μM); (b) change in F/F_0 for DP1 as a function of $[Cu(II)]_{tot}/[DP1]_{tot}$ concentration: 2.0 μM (red) and 0.2 μM (blue in 0.5 mM buffer). The solid traces are fitting curves of the experimental data to eqn (4), providing apparent $\log K_D' = -8.0 \pm 0.1$; (c) recovery of F/F_0 for $Cu^{II}_{0.8}$–DP1 (2.0 μM) with increasing concentration of competing ligand Gly; (d) curve fitting of $[Cu^{II}\text{–DP1}]/[DP1]_{tot}$ *versus* $\log[Cu_{aq}^{2+}]$ to eqn (8), providing conditional $\log K_D = -8.1 \pm 0.2$ for Cu^{II}–DP1.

a His residue in the third position; (iii) two intervening secondary amine peptide nitrogens.[36]

The other three probe complexes Cu^{II}–DP1–3 also exhibit similar peaks ($\varepsilon < 100\ M^{-1}\ cm^{-1}$) but at longer wavelengths (600–650 nm; Fig. 2). The behaviour is consistent with the presence of a type II Cu(II) centre in each complex. Similar d–d transitions were observed for Cu^{II}–GHK (Fig. 2) and Cu^{II}–PcoC.[30]

When excited at ~330 nm, the dansyl fluorophore in each DP probe in solution emits intense fluorescence at λ_{max} ~ 550 nm (Fig. 4a). Titration with Cu_{aq}^{2+} quenches the fluorescence intensity linearly until one equiv. of Cu(II) is added, suggesting that each probe binds one equiv. of Cu(II) preferentially (Fig. 4a and b; Fig. S2, ESI†). However, at sub-micromolar probe concentrations, the turning point of the titration curve for DP1 is lost (Fig. 4b), consistent with relatively weak Cu(II) binding. Titration of excess of a strong Cu(II) chelator such as Edta into solutions of each Cu^{II}–DP complex recovered the fluorescence intensity to that of the original metal-free form, consistent with the reversibility of Cu(II) binding and negligible inner-filter effects from other solution components. The absorbance at 326 nm can be attributed solely to the dansyl group (compare spectra of Cu^{II}–DP complexes *versus* Cu^{II}–DAHK in Fig. 2). The evidence suggests that the fluorescence quenching induced by Cu(II) binding arises primarily through paramagnetic interactions between the Cu(II) centre and the attached dansyl fluorophore, consistent with the previous observation of little change in absorbance at 326 nm upon Cu(II) binding (Fig. 2). This validates application of eqn (5) to the Cu(II) speciation analysis for the competing equilibriums of eqn (6) and (9) as there is no need to consider the possible inner-filter effects of the non-chromophoric ligands and metal ions. The system provides an excellent opportunity to develop a series of probes covering a range of affinities for Cu(II). Four such probes were developed in this work and are presented below, together with a brief comparison with our previous probe Aβ16wwa.

Probe DP1. It is a penta-peptide Ac-DH(K^{DNS})HD with N-terminal nitrogen acetylation and dansyl attached to the Lys3 side-chain (Fig. 1). Acetylating the N-terminal amine produces a probe of weaker affinity for Cu(II). Possible ligands include the carboxylate side-chains of Asp1 and Asp5, the imidazole side-chains of His2 and His4 and, at higher pH values, deprotonated peptide nitrogen(s). The methods outlined in the Experimental section applied to DP1 at low micromolar concentration range indicated a Cu(II) binding equilibrium at Cu : DP1 ~ 1 : 1 (Fig. 4b; eqn (1)) at pH 7.4 (MOPS buffer ≤ 5.0 mM) and provided an estimate of the apparent $\log K_D' = -8.0 \pm 0.1$ and specific F_1/F_0 values (Tables 1 and 2). It was also possible to determine a conditional $\log K_D = -8.1 \pm 0.2$ at pH 7.4 for Cu^{II}–DP1 *via* ligand competition using Gly as a competing affinity standard (Fig. 4c and d), based on reported data given in Table S1 (ESI†). The consistency of these two independent approaches confirms negligible buffer effects under the experimental conditions and the reliability of the K_D value determined for Cu(II)–DP1 here. This claim is consolidated by the fact that both probes DP1 and DP2 compete effectively for Cu(II) with the Ac-Aβ16 peptide and provide consistent outcomes (*vide infra*). Further details are given in the ESI.†

An equivalent analysis in CHES buffer (5.0 mM, pH 9.2) provided $\log K_D = -11.6 \pm 0.1$ for Cu^{II}–DP1 (Table 2). In addition, the fluorescence titration experiments revealed different F_1/F_0 values in the two buffers (Table 1). It is apparent that the Cu(II) binding site at pH 9.2 is different from that at pH 7.4. It is likely that, at higher pH, one or two deprotonated amides of the peptide links of His2 and/or His4 are involved in Cu(II) binding (*cf.*, the coordination mode of His3 in Fig. 3b). Further $\log K_D$ estimates at pH 8.0 and 8.5 are included in Table S2 (ESI†).

Probe DP2. This octa-peptide probe (DAE(K^{DNS})RHDH) was modified from the Aβ(1–8) sequence (DAEFRHDS) with Phe4 replaced by dansylated Lys and Ser8 by His (Fig. 1). The aim was to mimic the Cu(II) binding property of the Aβ16wwa probe reported recently,[20] and to provide a probe with an affinity somewhat higher than that of DP1.

Titration of Cu_{aq}^{2+} into solutions of DP2 (2.0 and 10 μM) in MOPS buffer (50 mM, pH 7.4) induced a linear quenching with a clear turning point at one equiv. of Cu_{aq}^{2+} but further minor quenching was apparent at higher Cu : probe ratios (Fig. 5a). There appears to be one higher affinity binding site with one or more sites of lower affinity, as observed previously for the Aβ16wwa probe.[20]

The affinity of the first site is too high (K_D too small) to be determined *via* direct metal ion titration due to the detection limit of the probe concentration (~0.1 μM). Consequently, the

Table 2 Conditional dissociation constants ($\log K_D$) of Cu^{II}-probe complexes

Complex	$\log K_D$ [a] pH 6.2	pH 7.4	pH 9.2	Affinity std	Ref.
Cu^{II}–DP1	—	−8.0(2)[b,c]	—	'H_2O'	Fig. 4a and b
	—	−8.1(2)[c]	−11.6(1)	Gly	Fig. 4c and d
Cu^{II}–DP2	−8.0(1)[c]	−10.1(1)	−12.5(1)	Gly	Fig. 5b and c
	−8.0(1)[c]	−10.0(1)	−12.4(1)	His	Fig. 5b and d
Cu^{II}–DP3	−10.2(1)	−12.4(1)	−13.4(1)	Gly	Fig. S4a and b (ESI)
	−9.9(1)	−12.2(1)	−13.4(1)	His	Fig. S4a and c (ESI)
Cu^{II}–DP4	−10.7(2)	−14.1(1)	−18.0(2)	His	Fig. S5a and b (ESI)
	−11.4(3)	−14.1(1)	−18.0(1)	Egta	Fig. S5a and c (ESI)
Cu^{II}–Aβ16wwa	−7.7(1)	−9.9(1)	−12.5(1)	DP2	Fig. S6c and d (ESI)
	−7.9(2)[b,c]	—	—	'H_2O'	Fig. S6a and b (ESI)
	—	−9.8(2)[d]	—	Gly	20

[a] Unless stated otherwise, the $\log K_D$ data were determined *via* ligand competition for Cu(II) between each probe and the specified affinity standard in respective buffer (50 mM) of MES (pH 6.2), MOPS (pH 7.4) and CHES (pH 9.2). The values in brackets refer to estimated deviations based on the quality of curve-fittings of the experimental data (see Fig. 4 and 5; Fig. S4–S6, ESI). [b] Apparent $\log K_D$ determined *via* direct metal ion titration. [c] Determined in diluted buffers (5.0 mM MOPS for 2.0 μM DP1 and 0.5 mM MOPS for 0.20 μM DP1) to minimize possible buffer competition for Cu(II) with the weak binding site. [d] Determined previously with fluorescence emission of Trp in Aβ16wwa as detection probe.

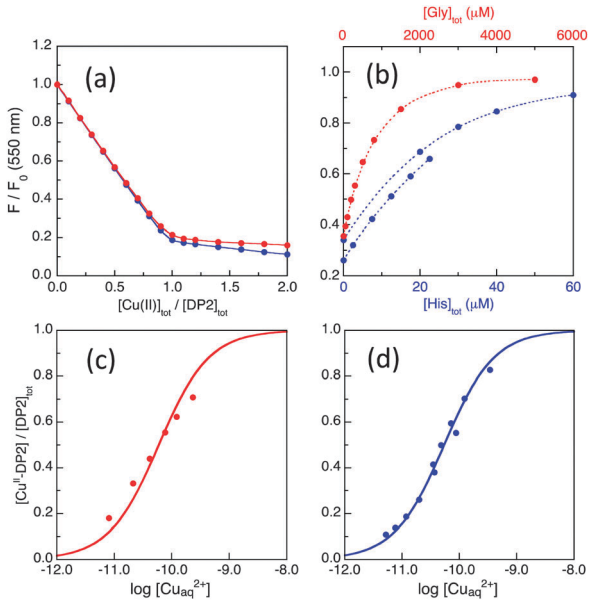

Fig. 5 Determination of conditional K_D for Cu^{II}–DP2 by competition with ligand Gly or His in MOPS buffer (50 mM, pH 7.4): (a) comparison of the titration curves for DP2 at 2.0 μM (red) and 10.0 μM (blue); (b) recovery of F(550) of $Cu^{II}_{0.8}$–DP2 or Cu^{II}–DP2 (10 μM) with increasing concentration of competing ligand Gly (in red on top scale) or His (in blue on bottom scale); (c, d) curve fittings of $[Cu^{II}–DP2]/[DP2]_{tot}$ *versus* $\log[Cu_{aq}^{2+}]$ to eqn (8) derived an consistent estimate of $\log K_D = -10.1 \pm 0.1$ for Cu^{II}–DP2 with either competing ligand Gly (c) or His (d).

affinity was determined *via* ligand competition with both Gly and His as affinity standards (Fig. 5b and c), as described for DP1 (see ESI†). Both analyses provided $\log K_D = -10.1 \pm 0.1$ at pH 7.4, an affinity higher by two orders of magnitude than that of DP1 (Table 2).

Equivalent experiments were conducted at lower and higher pH values in buffers MES (50 mM, pH 6.2) and CHES (50 mM, pH 9.2) (see ESI†). The derived affinities were 2 orders of magnitude lower at pH 6.2 and 2–3 orders of magnitude higher at pH 9.2 (Table 2). These observations are consistent with competition between Cu(II) and protons at pH 6.2 for the N-terminal nitrogen (pK_a = 8.0–8.5) as well as the two His ligands ($pK_a \sim 6.5$) and the involvement of at least one peptide backbone amido ligand at pH 9.2. Further $\log K_D$ estimates at other pH values are provided in Table S2 (ESI†).

Supporting evidence is provided by the characteristic F_1/F_0 values being different in the solutions at lower and higher pH (Table 1). The spectroscopic evidence supports a Cu(II) binding site transition similar to that which occurs for the Aβ16 peptide at pH ~ 7.8.[38] The Aβ16 peptide itself and its derivative Aβ16wwa possess comparable Cu(II) affinities and similar pH dependencies to that of DP2 (*vide infra*). Confirming characterisation of Aβ16wwa *via* DP2 is included in the ESI.†

Probe DP3. This is a hepta-peptide probe with a sequence of $HP(K^{DNS})DHDH$ (Fig. 1), designed for a higher affinity than DP2. A His residue was placed in position 1, aiming to provide a stabilising bidentate ligand *via* the sidechain and N-terminus (Fig. 3a). A proline residue was placed in position 2 to prevent that amide from acting as a ligand (*cf.*, Fig. 3b). His5 and His7 are expected to provide further ligands. Two negatively charged Asp residues were installed in the positions 4 and 6 to increase the ionization energy of the peptide bond amine hydrogens and discourage their participation as ligands. The probe binds Cu(II) with an affinity about two orders of magnitude stronger than DP2 at pH 7.4 (Table 2; Fig. S4 and Table S2, ESI†).

The characterisation data are consistent with the tetragonal site shown in Fig. 3a: (i) the complex Cu^{II}–DP3 eluted before *apo*-DP3 from an analytical anion exchange column equilibrated at pH 7.4 (Fig. 6), indicating that Cu(II) binding leads to a net gain of cationic charge, consistent with ionisation of the single N-terminal nitrogen only; (ii) DP3 is the only probe among the four whose $\log K_D$ at various pH within the range 6.2–9.2 can be fitted satisfactorily to eqn (S2) (ESI†) (see footnote of Table S1, ESI†) assuming a Cu(II) site of $\{–NH_2, 3N^{Im}(His)\}$ (Fig. 7). The derived parameters are the expected values: $\log({}^{abs}K_D) = -13.6$ for the pH-independent absolute dissociation constant; pK_a = 8.8 for the N-terminal amine; an average pK_a = 6.5 for the three His side-chains. Apparently, the Cu(II) site in

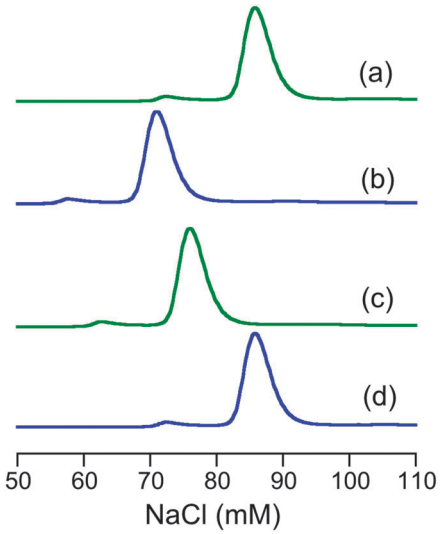

Fig. 6 Relative elution positions of *apo*- and Cu(II)-forms of DP3 and DP4 from an analytical anion-exchange column Resource™ Q (GE Life Sciences) in MOPS buffer (50 mM, pH 7.4): (a) *apo*-DP3; (b) Cu^{II}–DP3; (c) *apo*-DP4; (d) Cu^{II}–DP4. The elution was detected at 280 nm.

DP3 lacks peptide nitrogen anionic ligands with $pK_a > 9.2$ within the pH range 6.2–9.2. Notably, DP3 binds Cu(II) with an unchanged quenching index $F_1/F_0 = 0.13$ (Table 1) and the Cu(II)–DP3 complex displays an indistinguishable EPR spectrum (Fig. S7 and Table S3, ESI†) within the pH range 6.2–9.2, suggesting a uniform Cu(II) site. The carboxylate side-chains of Asp4 and/or Asp6 may contribute as axial ligand(s) but will have little impact on the pH dependency of $\log K_D$ at pH > 6 and on the EPR spectrum. They are sensitive to equatorial ligands only.

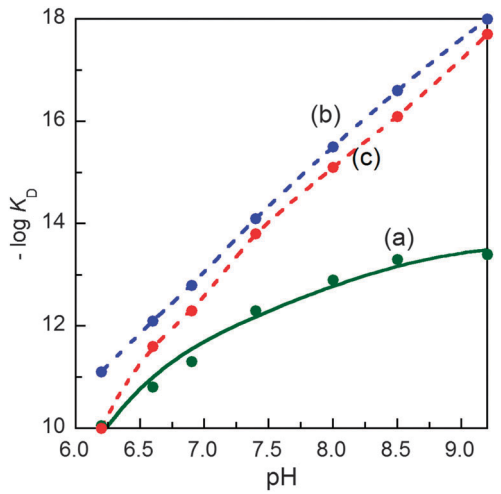

Fig. 7 Variation of conditional dissociation constant pK_D (= $-\log K_D$) with solution pH for Cu(II) complexes of: (a) DP3; (b) DP4 and (c) DAHK. The solid trace in (a) showed the best fit of the experimental data to eqn (S2) (ESI†) based on a metal binding site of {$-NH_2$, $3N^{Im}$(His)} in DP3 with the derived parameters $\log({}^{abs}K_D) = -13.6$, $pK_a = 8.8$ for $-NH_2$ and an average $pK_a = 6.5$ for the three N^{Im}(His). The dashed traces in (b, c) are the simple interpolations of the experimental data points for DP4 and DAHK ligands since the data cannot be fitted to eqn (S2) (ESI†) within the pH window.

Probe DP4. This tetra-peptide probe $H(K^{DNS})HH$ consists of three His and a dansylated Lys in position 2 (Fig. 1). It was designed originally to bind Cu(II) with a similar binding site to DP3 but with higher affinity. Indeed, it does bind Cu(II) with higher affinity than DP3 but also with much higher sensitivity to solution pH within the pH window 6.2–9.2 (Fig. 7b *vs.* 7a). This suggests that the Cu(II) site in DP4 involves at least one metal ligand with $pK_a > 9.2$. Consequently, it was necessary to recruit the higher affinity Cu(II) ligands Egta and Hedta (Table S1, ESI†) in addition to free His to estimate the affinity of DP4 in the pH range 6.2–9.2. The representative experiments are shown in Fig. S5 (ESI†), Fig. 10d and the results given in Tables 2 and 3; Table S2 (ESI†) and Fig. 7b.

The observed high pH dependency of $\log K_D$ beyond pH 9.2 is not compatible with a DP3-type binding mode for Cu(II). Further experimental evidence, with controls consisting of the ATCUN ligand DAHK[37] and the non-ATCUN ligand DP3 (*vide supra*), confirm that DP4 binds Cu(II) in the classic ATCUN binding mode, as shown in Fig. 3b. A full documentation is provided in the ESI.†

Application of the probes

The four DP probes developed in this work are able to quantify Cu(II) binding properties of target proteins and peptides in the extended range from micromolar to femtomolar (Fig. 8). Their individual binding sites differ and so do the dependencies of $\log K_D$ on solution pH (Table 2 and Table S2, ESI†).

Their potential of application was tested on a range of well-characterised targets. Results are summarised in Fig. 9 and 10 and Table 3. For example, the Cu(II) binding stoichiometries of peptides Aβ16, GHK and DAHK were determined by Cu_{aq}^{2+} titration of a mixture containing equal molar concentrations of each target peptide and DP2, as detailed for Aβ16 and DAHK in Fig. 9. It is apparent that the latter peptide exhibits a single site of highest affinity for Cu(II).

To quantify affinities, a protein or peptide target was titrated into a solution containing the appropriate probe complex Cu^{II}–DP to initiate an effective competition for Cu(II) according to eqn (9). The solution was monitored for recovery of probe fluorescence intensity according to eqn (5) (see Fig. 10, top panel). This allowed Cu(II) speciation analysis to determine a correlation between $[Cu^{II}–DP]$ and $[target]_{tot}/[DP]_{tot}$ that was fitted to eqn (11) to allow estimation of $\log K_D$ for the target from the known $\log K_D$ for the probe complex (Fig. 10, bottom panel; see Experimental section for details).

As the sensitive ranges of the probes overlap (Fig. 8), the affinities of many targets listed in Table 3 were consolidated with two different DP probes, highlighting the internal consistency of the approach. For example, both DP2 and DP3 provided estimates of $\log K_D$ for Aβ16 at pH 7.4 that were the same within experimental error to our previous value determined with the Aβ16wwa probe (Table 3). Acetylation of the N-terminus of Aβ16 leads to a decrease in affinity of ~2 orders of magnitude, as confirmed with both DP1 and DP2. This confirms the key role of the N-terminal amine in Cu(II) binding. Variation of $\log K_D$ with pH for Aβ16 is similar to that of DP2 within the whole pH range 6.2–9.2. It is comparable also to that of DP3 between

Table 3 Comparison of log K_D for selected Cu(II) complexes determined with the set of four DP probes to those reported previously

Complex	log K_D [a] pH 6.2	pH 7.4	pH 9.2	Reported log K_D at pH 7.4 unless otherwise indicated	Probe – affinity std	Ref.
Cu^{II}–PcoC–H1F		−8.2(2)			DP1 – Gly	This work
				≥ −6[b]	PcoC – 'H_2O'	30
Cu^{II}–AcAβ16		−8.1(1)			DP1 – Gly	This work
		−8.4(1)			DP2 – Gly/His	This work
				−8.3	Aβ16wwa–Gly	20
Cu^{II}–Aβ16	−8.2(1)	−10.2(1)	−12.5(1)		DP2 – Gly/His	This work
	−8.1(1)	−10.1(1)	−12.3(2)		DP3 – Gly/His	This work
				−10.0	Aβ16wwa–Gly	20
Cu^{II}–CopC	−12.3(2)	−13.7(1)			DP4 – His/Egta	This work
				−13.1[c]	CopC – Egta	29
Cu^{II}–PcoC	−11.3(3)	−13.5(3)	−14.0(3)		DP3 – Gly/His	This work
	−11.5(3)	−13.5(1)			DP4 – His/Egta	This work
				−13.2[c]	PcoC – Egta	30
GHK	−10.4(1)	−13.4(2)			DP3 – Gly/His	This work
	−10.4(1)	−13.3(2)	−16.3(2)		DP4 – His/Egta	This work
				−13.2	ITC – Gly	33
				−13.0	Potentiometry	41
DAHK	−10.0(1)	−13.8(2)	−17.7(2)		DP4 – His/Egta	This work
				−13.6	ITC – Gly	33
				−13.8	Potentiometry	42
Cu^{II}–Hedta	< −13[d]	−15.2(3)	−16.8(1)		DP4 – His/Egta	This work
	−13.7		−16.7	−14.9		44

[a] Unless stated otherwise, the log K_D data reported in this work were determined *via* ligand competition for Cu(II) between each probe with affinity given in Table 2 and the specified Cu(II)-binding Target in respective buffer (50 mM) of MES (pH 6.2), MOPS (pH 7.4) and CHES (pH 9.2). The bracketed values refer to estimated deviations based on the quality of curve-fitting of the experimental data (*cf.* Fig. 10). [b] Apparent affinity estimated *via* direct metal ion titration in KPi buffer (pH 7.0). [c] Values determined in KPi buffer at pH 7.0. [d] The affinity difference between DP4 and Hedta at pH 6.2 is too large to allow reliable estimation.

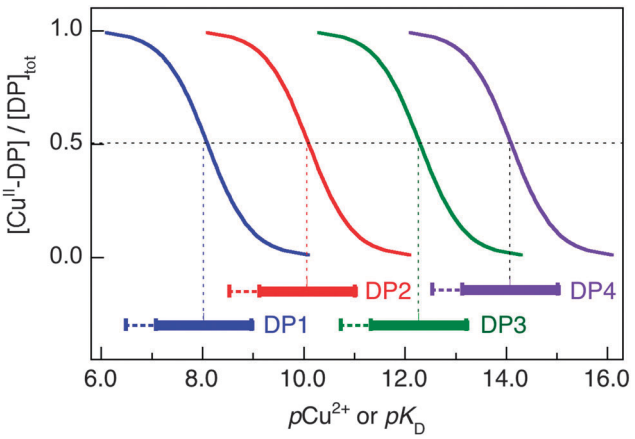

Fig. 8 Buffer range for [Cu_{aq}^{2+}] (expressed as pCu^{2+}) of the four DP probes in MOPS buffer at pH 7.4 for determining the target peptide/protein Cu(II) affinity (expressed as pK_D). The buffering range is calculated based on 10–90% Cu(II) occupancy on each DP probe and log K_D = −8.1, −10.1, −12.3 and −14.1 at pH 7.4 for DP1, DP2, DP3 and DP4, respectively. Extension for determining pK_D to weaker (but not stronger) affinity range is decided by a restriction of the determination approach that allows variation of the target concentration, but not the DP probe concentration.

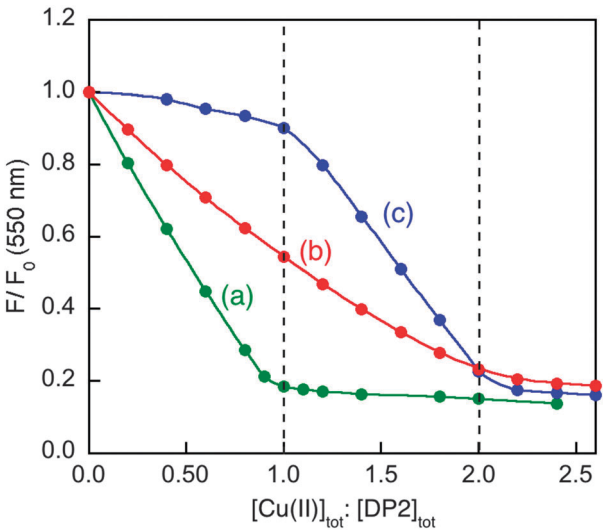

Fig. 9 Determination of Cu(II) binding stoichiometry in MOPS buffer (50 mM, pH 7.4) *via* titration with Cu_{aq}^{2+} of: (a) DP2 probe (2.0 μM) only; (b) a 1 : 1 mixture of DP2 and Aβ16 (each 2.0 μM); (c) a mixture of DP2 and peptide DAHK (each 2.0 μM).

pH 6.2–7.4, but very different between pH 7.4–9.2 (Table 3). This is consistent with a Cu(II) site transition in Aβ16 with a peptide amide nitrogen anionic ligand contributing to Cu(II) coordination at pH > 7.4, but not at pH < 7.4 (*vide supra*).[38]

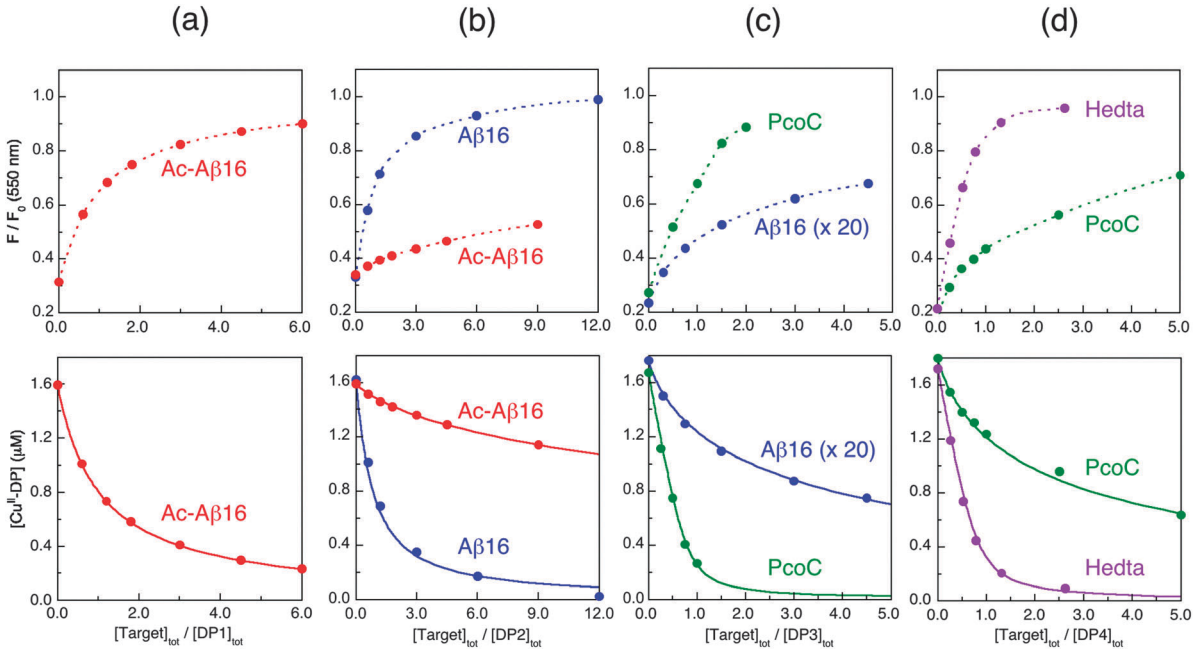

Fig. 10 Determination of conditional K_D for various protein/peptide targets in MOPS buffer (50 mM, pH 7.4): (a) Ac-Aβ16 with DP1 probe; (b) Ac-Aβ16 and Aβ16 with DP2 probe; (c) Aβ16 (note: 20× conc.) and PcoC with DP3 probe; (d) PcoC and Hedta with DP4 probe. Top panel showed recovering of the DP fluorescence intensity upon titration of each Cu^{II}_x–DP complex (x = 0.8–0.9) with related competing Target ligands where the dot traces are the simple interpolations of the experimental points, and bottom panel gave correlation of [Cu^{II}–DP] *versus* $[target]_{tot}/[DP]tot$ where the solid traces are the fitting curves of the experimental data to eqn (11) that allowed determination of conditional K_D for each peptide/protein target as given in Table 3.

CopC and PcoC are two copper binding proteins expressed to the periplasmic space of two different copper-resistant Gram-negative bacteria.[39,40] They share highly conserved protein sequences, protein structures and metal-binding sites. They each feature two separated copper-binding sites specific, respectively, for Cu(I) and Cu(II).[29,30] The affinities of their Cu(II) sites at pH 7.4 were determined, again indistinguishably, with the DP3 and DP4 probes. These values ($\log K_D = -13.7$ and -13.5 at pH 7.4) are consistent with previous estimates ($\log K_D = -13.1$ and -13.2 at pH 7.0).[30] Variation of $\log K_D$ with pH is somewhat comparable to that of DP3 (Table 4), consistent with the similarity of their Cu(II) binding sites (Fig. 3a). The Cu(II) site in CopC comprises a bidentate His1 ligand, the side-chain of His90 and a possible H_2O molecule or a carboxylate side-chain as the fourth coordination ligand.[29] Consequently, mutation of His1 to Phe1 decreases the Cu(II) affinity by more than five orders of magnitude, as determined in this work with probe DP1 (Table 3). A conserved proline residue in the second position of both protein sequences promotes the DP3 binding mode and prevents the DP4 ATCUN binding mode (Fig. 3).

Peptides GHK and DAHK are naturally-occurring Cu(II)-binding peptides present in human serum and cerebrospinal fluid.[36] Their Cu(II) binding affinities were determined previously by classic potentiometric titration at $\log K_D = -13.0$

Table 4 Experimental evidences for possible peptide amide nitrogen (N^-) binding to Cu(II)

Complex	λ_{max} (nm)/ε_{max} (M^{-1} cm^{-1}) for Cu^{II}(d–d)[a]	$\Delta(Q^-)$ upon Cu^{II} binding at pH 7.4[b]	$\Delta(\log K_D)$ with pH		(N^-)–Cu^{II} at pH	
			6.2 → 7.4	7.4 → 9.2	7.4	9.2
Cu^{II}–DP1	~650/~30	—	—	3.5	??	Yes
Cu^{II}–DP2	625/70	—	2.1	2.4	No	Yes
Cu^{II}–DP3	~600/~45	Decrease	2.2	1.1	No	No
Cu^{II}–DP4	525/120	Increase	3.0	3.9	Yes	Yes
Cu^{II}–Aβ16	625/80	—	2.0	2.3	No	Yes
Cu^{II}–PcoC	610/110[c]	Decrease[c,d]	2.1	0.5	No	No
Cu^{II}–GHK	625/50	—	3.0	3.0	Yes	Yes
Cu^{II}–DAHK	525/100	—	3.8	3.9	Yes	Yes
Cu^{II}–(Egta)			2.4[e]	3.0[e]		
Cu^{II}–(Hedta)			1.3[e]	1.4[e]		

[a] Solution spectra recorded in MOPS buffer at pH 7.4 (see Fig. 2). [b] Change in net negative charge (Q^-) upon formation of each Cu(II) complex was evaluated by comparative elution, from an analytical anion-exchange column, of metal-free and metal-bound forms of each peptide/protein molecule (see Fig. 6). [c] Quoted from ref. 30. [d] Increase in net positive charge upon Cu(II) binding as evidenced from comparative elution from a cation-exchange column. [e] Quoted from data in Table S1 (ESI).

and −13.8, respectively.[41,42] Both values were confirmed more recently by independent ITC approach with $[Cu^{II}(Gly)_2]$ stabilized by excess Gly at high concentrations from 2.8 mM to 50 mM ($\log K_D$ = −13.2 and −13.6).[33] This work supported these values ($\log K_D$ = −13.3 and −13.8) but with the simpler approach of ligand competition with the probe DP4 (Table 3). Furthermore, we confirm readily that the Cu(II) affinities of both peptides are highly pH-sensitive within the range pH 6.2–9.2 (Tables 3 and 4 and Fig. 7), consistent with peptide amide nitrogen(s) acting as key ligand(s).[37] Interestingly, at pH 7.4, the Cu(II) affinities of DAHK ($\log K_D$ = −13.8)[42] and the C-terminal amidated DAH-NH_2 ($\log K_D$ = −13.7)[43] are only marginally weaker than the Cu(II) affinity of our DP4 probe ($\log K_D$ = −14.2; sequence $H(K^{DNS})HH$), supporting the proposed Cu(II) site in DP4 of Fig. 3b with a minimal contribution from the side-chains of His1 and His4 as possible axial ligand(s) only.

Last but not least, the Cu(II) affinity of a well-documented classic Cu(II) ligand Hedta was checked with the DP4 probe (Fig. 10d). Although the affinity of Hedta at pH 6.2 is too high to be accessed by the DP4 probe, the data acquired at pH 7.4 and 9.2 match the literature values (Table 3). This is a further endorsement of the reliability and robustness of the four DP probes developed in this work.

Concluding remarks

A set of four highly sensitive fluorescent probes DP1–4 were developed and established in this work. They were demonstrated to be a set of robust and complementary probes capable of exploring the Cu(II) chemistry of proteins and peptides. Each of the probes binds one equivalent of Cu(II) cleanly with minimal formation of ternary complexes with competing ligands, a pre-condition for determination of metal affinity by ligand competition (Fig. S2, ESI†). The probes were designed to display affinities in the micromolar to femtomolar concentration ranges at pH 7.4 (Table 2). The affinities were calibrated carefully in each case with at least two well-documented and independent affinity standards (Gly, His, Egta, Hedta) and were cross-checked directly or indirectly with other independent approaches such as direct metal ion titration, ITC and potentiometry (Tables 2 and 3).

Similar to most other Cu(II) binding molecules, the affinities of the four DP probes are pH-dependent, as summarised in Table 4 and so great care must be excised to control the correct solution pH when these probes are used. On the other hand, a detailed comparison between the differences in such pH dependency among the four DP probes, plus other evidence, provides valuable information of the nature of the different Cu(II) sites in DP1–4 (*cf.*, Fig. 3). Overall, this system provides a valuable platform to explore Cu(II) binding targets, as exemplified by Table 4.

Acknowledgements

This work was supported by fund from the Australian Research Council under grant DP130100728. We thank Mrs Sioe See Volaric (University of Melbourne) for providing technical support for recording EPR spectra.

Notes and references

1 R. A. Festa and D. J. Thiele, Copper: An essential metal in biology, *Curr. Biol.*, 2011, **21**, R877–R883.
2 S. Lutsenko, Human copper homeostasis: a network of interconnected pathways, *Curr. Opin. Chem. Biol.*, 2010, **14**, 211–217.
3 N. J. Robinson and D. R. Winge, Copper metallochaperones, *Annu. Rev. Biochem.*, 2010, **79**, 537–562.
4 S. Tottey, C. J. Patterson, L. Banci, I. Bertini, I. C. Felli, A. Pavelkova, S. J. Dainty, R. Pernil, K. J. Waldron, A. W. Foster and N. J. Robinson, Cyanobacterial metallochaperone inhibits deleterious side reactions of copper, *Proc. Natl. Acad. Sci. U. S. A.*, 2012, **109**, 95–100.
5 J. F. Mercer, The molecular basis of copper-transport diseases, *Trends Mol. Med.*, 2001, **7**, 64–69.
6 K. J. Barnham, C. L. Masters and A. I. Bush, Neurodegenerative diseases and oxidative stress, *Nat. Rev. Drug Discovery*, 2004, **3**, 205–214.
7 P. S. Donnelly, Z. Xiao and A. G. Wedd, Copper and Alzheimer's disease, *Curr. Opin. Chem. Biol.*, 2007, **11**, 128–133.
8 E. Gaggelli, H. Kozlowski, D. Valensin and G. Valensin, Copper homeostasis and neurodegenerative disorders (Alzheimer's, prion, and Parkinson's diseases and amyotrophic lateral sclerosis), *Chem. Rev.*, 2006, **106**, 1995–2044.
9 D. J. Waggoner, T. B. Bartnikas and J. D. Gitlin, The role of copper in neurodegenerative disease, *Neurobiol. Dis.*, 1999, **6**, 221–230.
10 Z. Xiao and A. G. Wedd, The challenges of determining metal-protein affinities, *Nat. Prod. Rep.*, 2010, **27**, 768–789.
11 Z. Xiao, F. Loughlin, G. N. George, G. J. Howlett and A. G. Wedd, C-terminal domain of the membrane copper transporter Ctr1 from Saccharomyces cerevisiae binds four Cu(I) ions as a cuprous-thiolate polynuclear cluster: sub-femtomolar Cu(I) affinity of three proteins involved in copper trafficking, *J. Am. Chem. Soc.*, 2004, **126**, 3081–3090.
12 Z. Xiao, P. S. Donnelly, M. Zimmermann and A. G. Wedd, Transfer of Copper between Bis(thiosemicarbazone) Ligands and Intracellular Copper-Binding Proteins. Insights into Mechanisms of Copper Uptake and Hypoxia Selectivity, *Inorg. Chem.*, 2008, **47**, 4338–4347.
13 Z. Xiao, J. Brose, S. Schimo, S. M. Ackland, S. La Fontaine and A. G. Wedd, Unification of the copper(I) binding affinities of the metallo-chaperones Atx1, Atox1 and related proteins: detection probes and affinity standards, *J. Biol. Chem.*, 2011, **286**, 11047–11055.
14 P. Bagchi, M. T. Morgan, J. Bacsa and C. J. Fahrni, Robust Affinity Standards for Cu(I) Biochemistry, *J. Am. Chem. Soc.*, 2013, **135**, 18549–18559.
15 Z. Xiao, L. Gottschlich, R. van der Meulen, S. R. Udagedara and A. G. Wedd, Evaluation of quantitative probes for

weaker Cu(I) binding sites completes a set of four capable of detecting Cu(I) affinities from nanomolar to attomolar, *Metallomics*, 2013, **5**, 501–513.

16 C. J. Fahrni, Synthetic fluorescent probes for monovalent copper, *Curr. Opin. Chem. Biol.*, 2013, **17**, 656–662.

17 I. Zawisza, M. Rózga and W. Bal, Affinity of copper and zinc ions to proteins and peptides related to neurodegenerative conditions (Aβ, APP, α-synuclein, PrP), *Coord. Chem. Rev.*, 2012, **256**, 2297–2307.

18 N. E. Grossoehme, A. M. Spuches and D. E. Wilcox, Application of isothermal titration calorimetry in bioinorganic chemistry, *JBIC, J. Biol. Inorg. Chem.*, 2010, **15**, 1183–1191.

19 D. Jiang, L. Zhang, G. P. G. Grant, C. G. Dudzik, S. Chen, S. Patel, Y. Hao, G. L. Millhauser and F. Zhou, The Elevated Copper Binding Strength of Amyloid-β Aggregates Allows the Sequestration of Copper from Albumin: A Pathway to Accumulation of Copper in Senile Plaques, *Biochemistry*, 2012, **52**, 547–556.

20 T. R. Young, A. Kirchner, A. G. Wedd and Z. Xiao, An Integrated Study of the Affinities of the Aβ16 Peptide for Cu(I) and Cu(II): Implications for the Catalytic Production of Reactive Oxygen Species, *Metallomics*, 2014, **6**, 505–517.

21 Y. Jeong and J. Yoon, Recent progress on fluorescent chemosensors for metal ions, *Inorg. Chim. Acta*, 2012, **381**, 2–14.

22 M. Formica, V. Fusi, L. Giorgi and M. Micheloni, New fluorescent chemosensors for metal ions in solution, *Coord. Chem. Rev.*, 2012, **256**, 170–192.

23 Y. Zheng, K. M. Gattas-Asfura, V. Konka and R. M. Leblanc, A dansylated peptide for the selective detection of copper ions, *Chem. Commun.*, 2002, 2350–2351.

24 C. R. Lohani, J. M. Kim and K.-H. Lee, Two dansyl fluorophores bearing amino acid for monitoring Hg^{2+} in aqueous solution and live cells, *Tetrahedron*, 2011, **67**, 4130–4136.

25 L. N. Neupane, P. Thirupathi, S. Jang, M. J. Jang, J. H. Kim and K.-H. Lee, Highly selectively monitoring heavy and transition metal ions by a fluorescent sensor based on dipeptide, *Talanta*, 2011, **85**, 1566–1574.

26 B. Wang, H.-W. Li, Y. Gao, H. Zhang and Y. Wu, A Multifunctional Fluorescence Probe for the Detection of Cations in Aqueous Solution: the Versatility of Probes Based on Peptides, *J. Fluoresc.*, 2011, **21**, 1921–1931.

27 H.-H. Zeng, R. B. Thompson, B. P. Maliwal, G. R. Fones, J. W. Moffett and C. A. Fierke, Real-Time Determination of Picomolar Free Cu(II) in Seawater Using a Fluorescence-Based Fiber Optic Biosensor, *Anal. Chem.*, 2003, **75**, 6807–6812.

28 B. J. McCranor, H. Szmacinski, H. H. Zeng, A. K. Stoddard, T. Hurst, C. A. Fierke, J. R. Lakowicz and R. B. Thompson, Fluorescence lifetime imaging of physiological free Cu(II) levels in live cells with a Cu(II)-selective carbonic anhydrase-based biosensor, *Metallomics*, 2014, **6**, 1034–1042.

29 L. Zhang, M. Koay, M. J. Maher, Z. Xiao and A. G. Wedd, Intermolecular transfer of copper ions from the CopC protein of *Pseudomonas syringae*. Crystal structures of fully loaded Cu(I)Cu(II) forms, *J. Am. Chem. Soc.*, 2006, **128**, 5834–5850.

30 K. Y. Djoko, Z. Xiao, D. L. Huffman and A. G. Wedd, Conserved Mechanism of Copper Binding and Transfer. A Comparison of the Copper-Resistance Proteins PcoC from *Escherichia coli* and CopC from *Pseudomonas syringae*, *Inorg. Chem.*, 2007, **46**, 4560–4568.

31 G. Weber, Polarization of the fluorescence of macromolecules. II. Fluorescent conjugates of ovalbumin and bovine serum albumin, *Biochem. J.*, 1952, **51**, 155–167.

32 R. F. Chen, Dansyl labeled proteins: Determination of extinction coefficient and number of bound residues with radioactive dansyl chloride, *Anal. Biochem.*, 1968, **25**, 412–416.

33 A. Trapaidze, C. Hureau, W. Bal, M. Winterhalter and P. Faller, Thermodynamic study of Cu2+ binding to the DAHK and GHK peptides by isothermal titration calorimetry (ITC) with the weaker competitor glycine, *JBIC, J. Biol. Inorg. Chem.*, 2012, **17**, 37–47.

34 There is a minor fluorescence contribution at 550 nm from high concentration of histidine (>1 mM). To avoid such contribution, recovery of the fluorescence intensity was monitored at 600 nm when a high concentration (>1 mM) of histidine was needed as a competing ligand.

35 The higher intensity of the d–d transition at 525 nm for Cu^{II}–DP4 relative to that for Cu^{II}–DAHK is due to a background contribution of the dansyl absorbance in the former complex.

36 C. Harford and B. Sarkar, Amino Terminal Cu(II)- and Ni(II)-Binding Motif of Proteins and Peptides: Metal Binding, DNA Cleavage, and Other Properties, *Acc. Chem. Res.*, 1997, **30**, 123–130.

37 C. Hureau, H. Eury, R. Guillot, C. Bijani, S. Sayen, P.-L. Solari, E. Guillon, P. Faller and P. Dorlet, X-ray and Solution Structures of Cu^{II}–GHK and Cu^{II}–DAHK Complexes: Influence on Their Redox Properties, *Chem. – Eur. J.*, 2011, **17**, 10151–10160.

38 C. Hureau, Coordination of redox active metal ions to the amyloid precursor protein and to amyloid-β peptides involved in Alzheimer disease. Part 1: An overview, *Coord. Chem. Rev.*, 2012, **256**, 2164–2174.

39 D. A. Cooksey, Molecular mechanisms of copper resistance and accumulation in bacteria, *FEMS Microbiol. Rev.*, 1994, **14**, 381–386.

40 D. L. Huffman, J. Huyett, F. W. Outten, P. E. Doan, L. A. Finney, B. M. Hoffman and T. V. O'Halloran, Spectroscopy of Cu(II)-PcoC and the multicopper oxidase function of PcoA, two essential components of *Escherichia coli* pco copper resistance operon, *Biochemistry*, 2002, **41**, 10046–10055.

41 M. J. A. Rainer and B. M. Rode, The complex formation of copper(II) with GHL and HSA, *Inorg. Chim. Acta*, 1984, **92**, 1–7.

42 M. Sokolowska, A. Krezel, M. Dyba, Z. Szewczuk and W. Bal, Short peptides are not reliable models of thermodynamic and kinetic properties of the N-terminal metal binding site in serum albumin, *Eur. J. Biochem.*, 2002, **269**, 1323–1331.

43 K. S. Iyer, S. J. Lau, S. H. Laurie and B. Sarkar, Synthesis of the native copper(II)-transport site of human serum albumin and its copper(II)-binding properties, *Biochem. J.*, 1978, **169**, 61–69.

44 A. E. Martell and R. M. Smith, *NIST Critically Selected Stability Constants of Metal Complexes Database 46, Version 8.0*, U.S. Dept. of Commerce, NIST Standard Reference Data Program, Gaithersburg, MD, 2004.